

# Si(111)- $\alpha$ - $\sqrt{3} \times \sqrt{3}$ -Au phase modified by In adsorption: Stabilization of a homogeneous surface by stress relief

D. V. Gruznev,<sup>1,\*</sup> I. N. Filippov,<sup>2</sup> D. A. Olyanich,<sup>1</sup> D. N. Chubenko,<sup>3</sup> I. A. Kuyanov,<sup>1,2</sup> A. A. Saranin,<sup>1,2</sup>  
A. V. Zotov,<sup>1,2,3</sup> and V. G. Lifshits<sup>1,2,3</sup>

<sup>1</sup>*Institute of Automation and Control Processes, 690041 Vladivostok, Russia*

<sup>2</sup>*Faculty of Physics and Engineering, Far Eastern State University, 690000 Vladivostok, Russia*

<sup>3</sup>*Department of Electronics, Vladivostok State University of Economics and Service, 690600 Vladivostok, Russia*

(Received 11 November 2005; revised manuscript received 25 January 2006; published 27 March 2006)

Structural transformations on the Si(111)- $\alpha$ - $\sqrt{3} \times \sqrt{3}$ -Au surface induced by In adsorption have been studied using scanning tunneling microscopy and first-principles total-energy calculations. It has been found that In adsorption results in the transformation of the  $\sqrt{3} \times \sqrt{3}$ -Au phase to the  $\sqrt{3} \times \sqrt{3}$ -(Au,In) phase. At room temperature, the transformation is limited by the interior of the original  $\sqrt{3} \times \sqrt{3}$ -Au domains and does not affect the domain-wall structure. Upon annealing at 600 °C, the domain walls are eliminated and highly ordered almost defect-free homogeneous  $\sqrt{3} \times \sqrt{3}$ -(Au,In) surface develops. The  $\sqrt{3} \times \sqrt{3}$ -(Au,In) surface phase contains 1 monolayer (ML) of Au, 1 ML of Si and about 0.15 ML of In. Plausible mechanism of stabilization of the domain-wall-free Si(111)- $\sqrt{3} \times \sqrt{3}$ -(Au,In) surface is the stress relief caused by In adsorption.

DOI: 10.1103/PhysRevB.73.115335

PACS number(s): 68.35.Bs, 68.55.Jk, 68.37.Ef, 71.15.Nc

## I. INTRODUCTION

Among a variety of the metal-induced  $\sqrt{3} \times \sqrt{3}$ -R30° reconstructions on the Si(111) surface, the Si(111)- $\sqrt{3} \times \sqrt{3}$ -Au is the one, which peculiar features are associated with its domain-wall structure.<sup>1</sup> While atomic arrangement of the  $\sqrt{3} \times \sqrt{3}$ -Au phase within domains remains unchanged [for which the conjugate honeycomb-chained-trimer (CHCT) model<sup>2</sup> is considered to be the most plausible one], the density and structure of the domain walls evolve greatly, depending on the growth conditions. As a result, several types of surface structures are distinguished as follows. The surface with the minimal density of the domain walls is defined as  $\alpha$ - $\sqrt{3} \times \sqrt{3}$ -Au. With increasing Au coverage, the density of the domain walls grows and  $\alpha$ - $\sqrt{3} \times \sqrt{3}$ -Au continuously transforms into the  $\beta$ - $\sqrt{3} \times \sqrt{3}$ -Au with the maximal domain-wall density. It should be noted that both surfaces are observed at RT, since when they are heated to above 600 °C a high-temperature  $\gamma$ - $\sqrt{3} \times \sqrt{3}$  phase develops.<sup>1,3</sup> This surface is free of domain walls, but upon cooling to RT the domain walls reappear. For the surface with a low domain-wall density, the only  $\alpha$ - $\sqrt{3} \times \sqrt{3}$ -Au restores independent of the cooling rate. This is not the case for the surface with a high domain-wall density. The  $\beta$ - $\sqrt{3} \times \sqrt{3}$ -Au surface with a random domain-wall structure (“domain-wall glass”) is formed by quench cooling, while slow cooling produces a surface in which the ordered domain-wall structure with a  $6 \times 6$  periodicity (“domain-wall crystal”) develops.<sup>1,4,5</sup> The physics underlying the fascinating behavior of the domain walls in the Si(111)- $\sqrt{3} \times \sqrt{3}$ -Au remains an intriguing subject and demands further investigations.

In the present work, we have studied how In adsorption affects the reconstruction and domain-wall structure of the Si(111)- $\alpha$ - $\sqrt{3} \times \sqrt{3}$ -Au surface. In particular, it has been demonstrated that adsorption of about 0.4 monolayers (ML) of In followed by short annealing at about 600 °C, leaving

about 0.15 ML of In, produces at RT a highly ordered homogeneous Si(111)- $\sqrt{3} \times \sqrt{3}$ -(Au,In) surface free of domain walls. The plausible mechanism of the stabilization of the domain-wall-free Si(111)- $\sqrt{3} \times \sqrt{3}$ -(Au,In) surface is concluded to be stress relieving caused by In adsorption.

## II. EXPERIMENTAL AND CALCULATION DETAILS

Our experiments were performed with Omicron STM-VT25 operated in an ultrahigh vacuum ( $\sim 2.5 \times 10^{-10}$  mbar). Atomically clean Si(111)- $7 \times 7$  surfaces were prepared *in situ* by flashing to 1280 °C after the samples were first outgassed at 600 °C for several hours.<sup>6</sup> Gold was deposited from a heated Au-covered W wire at a rate of about 0.5 ML/min. Indium was deposited from a Ta foil tube at a rate of 0.01 ML/min. Deposition rates were evaluated from the scanning tunneling microscopy (STM) observations. For estimation of the Au deposition rate, the Si(111)- $\sqrt{3} \times \sqrt{3}$ -Au phase, which according to the CHCT model<sup>2</sup> has a coverage of 1 ML, was taken as a reference. The In deposition rate was accurately determined by counting the density of the six-atom magic In clusters formed at the early stages of In deposition onto the Si(111)- $7 \times 7$  surface,<sup>7</sup> as well as from the dose needed to form the  $\sqrt{3} \times \sqrt{3}$ -In surface phase with 1/3 ML of In. In the experiment, the Si(111)- $\alpha$ - $\sqrt{3} \times \sqrt{3}$ -Au surface was prepared by Au deposition at 700 °C in accordance with the Au/Si(111) phase diagram.<sup>8</sup> After cooling the sample to RT, from 0.01 to 0.5 ML of In was deposited onto the surface. Annealing of the sample was conducted at 600 °C, i.e., at temperature, where the  $\alpha$ - $\sqrt{3} \times \sqrt{3} \leftrightarrow \gamma$ - $\sqrt{3} \times \sqrt{3}$  phase transition takes place.<sup>1,3</sup> For STM observations, electrochemically etched tungsten tips cleaned by *in situ* heating were employed. The STM images were acquired in a constant-current mode after cooling the sample to room temperature.

The *ab initio* total-energy calculations were performed using the FHI96MD code<sup>9</sup> in which the Car-Parrinello type of electronic structure calculations<sup>10</sup> were used. The local density approximation (LDA) after Ceperley-Alder<sup>11</sup> in the Perdew-Zunger parametrization<sup>12</sup> for the exchange and correlation functional and fully separable Troullier-Martins<sup>13</sup> (for Au) and Hamann<sup>14</sup> (for Si and In) pseudopotentials have been employed. The pseudopotentials were constructed using the FHI98PP code<sup>15</sup> and were verified to avoid ghost states and to describe the basic experimental characteristic of bulk materials.

The surface has been simulated by a periodic slab geometry with a  $\sqrt{3} \times \sqrt{3}$  unit cell containing four silicon atomic bilayers and top Au-Si mixed bilayer. The dangling bonds of the bottom slab layer have been saturated by hydrogen atoms. The hydrogen atoms and bottom bilayer silicon atoms have been fixed and the rest atoms have been set free to move. A vacuum region of approximately 0.8 nm has been incorporated within each periodic unit cell to prevent interaction between adjacent surfaces. The energy cutoff of 35 Ry has been applied in all calculations presented.

### III. RESULTS AND DISCUSSION

#### A. Structural transformations of Si(111)- $\alpha$ - $\sqrt{3} \times \sqrt{3}$ -Au phase induced by In adsorption

Figure 1 shows STM images of the initial Si(111)- $\alpha$ - $\sqrt{3} \times \sqrt{3}$ -Au surface prior In deposition. In agreement with the earlier STM observations,<sup>1,16,17</sup> the surface shows up in the large-scale image as combination of the dark regions corresponding to the domains of the commensurate  $\sqrt{3} \times \sqrt{3}$ -Au phase and a network of the bright lines corresponding to the domain walls [indicated  $\sqrt{3}$  and DW, respectively, in Fig. 1(a)]. In the high-resolution STM images [Figs. 1(b) and 1(c)], one can see that the  $\sqrt{3} \times \sqrt{3}$ -Au domains appear as hexagonal arrays of the bright protrusions. Simulation of the STM images for the CHCT model indicates that these bright protrusions correspond to the centers of Au trimers which are located in  $T_4$  sites with respect to the first complete Si double layer.<sup>2</sup> Recall that according to the CHCT model Au trimers reside on the missing-top-layer Si(111) substrate. The neighboring  $\sqrt{3} \times \sqrt{3}$  domains are out of phase, which results in the occurrence of the antiphase domain walls. The domain walls have a shape of the polygonal lines with linear segments aligned along the  $[11\bar{2}]$ -type directions. As indicated in Figs. 1(b) and 1(c), the domain walls have a  $2 \times \sqrt{3}$  local periodicity, as they form by two edge rows of protrusions belonging to the two antiphase  $\sqrt{3} \times \sqrt{3}$  domains separated by a  $2a$ -wide gap. In the empty-state images, additional protrusions are seen approximately in the centers of the  $2 \times \sqrt{3}$  unit cells [see Fig. 1(b)]. These protrusions were interpreted in Ref. 17 as corresponding to the Au trimers, which are centered in the  $H_3$  sites and rotated by  $180^\circ$  with respect to the usual  $T_4$ -centered Au trimers (see Fig. 7). Local Au coverage in the domain walls is higher than that within the  $\sqrt{3} \times \sqrt{3}$  domains,<sup>1,17</sup> hence, these are so-called heavy domain walls. In the empty-state STM images, the domain walls have a greater apparent height than the interior

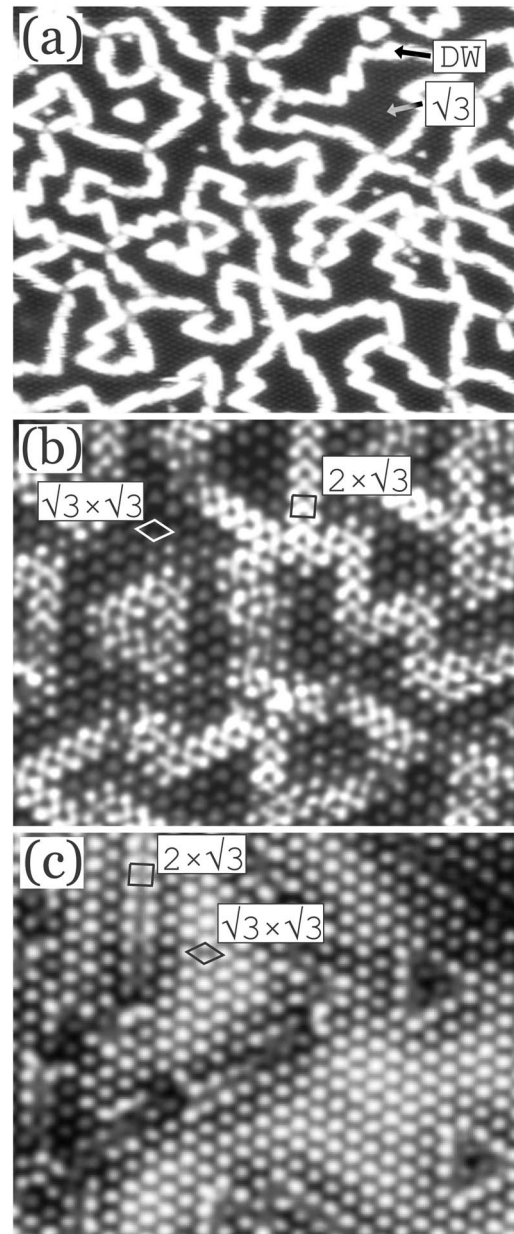


FIG. 1. STM images of the Si(111)- $\alpha$ - $\sqrt{3} \times \sqrt{3}$ -Au surface. (a)  $50 \times 40 \text{ nm}^2$  empty-state (+2.5 V) image; (b)  $16 \times 13 \text{ nm}^2$  empty-state (+0.8 V) image; (c)  $16 \times 13 \text{ nm}^2$  filled-state (-0.8 V) image. Images in (b) and (c) were taken from the different surface regions. Unit cells of the  $\sqrt{3} \times \sqrt{3}$  commensurate domains and of the  $2 \times \sqrt{3}$  domain walls are outlined.

of the domains, which is believed to be mainly due to the electronic effects.<sup>17</sup>

Room temperature adsorption of In onto the Si(111)- $\alpha$ - $\sqrt{3} \times \sqrt{3}$ -Au surface modifies its structure, as illustrated in Fig. 2. In the large-scale empty-state STM image [Fig. 2(a)], one can see that the structure of the domain-wall network is preserved, but the apparent-height contrast of the surface becomes reversed. Now the phase domains are seen brighter than the domain walls. The high-resolution STM images [Figs. 2(b) and 2(c)] demonstrate that the structure within phase domains has been changed significantly. While the

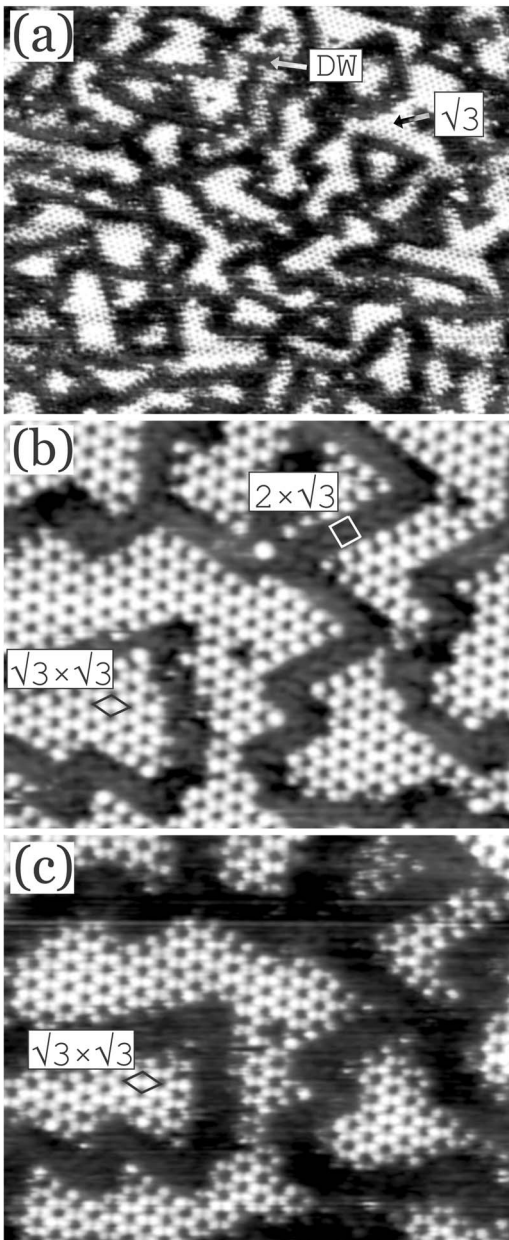


FIG. 2. STM images of the Si(111)- $\alpha$ - $\sqrt{3} \times \sqrt{3}$ -Au surface after RT deposition of 0.1 ML of In. (a)  $50 \times 40 \text{ nm}^2$  empty-state (+0.7 V) image; (b)  $16 \times 13 \text{ nm}^2$  empty-state (+0.8 V) image; and (c)  $16 \times 13 \text{ nm}^2$  filled-state (-0.8 V) image. Images in (b) and (c) were taken from the same surface area. The  $\sqrt{3} \times \sqrt{3}$  and  $2 \times \sqrt{3}$  unit cells are outlined.

$\sqrt{3} \times \sqrt{3}$ -Au phase shows up in STM images as a hexagonal array of protrusions, the  $\sqrt{3} \times \sqrt{3}$ -(Au,In) phase displays a honeycomblike structure. As for the domain walls, their close inspection has revealed that they are preserved essentially unchanged [even the presence of the additional protrusion within the  $2 \times \sqrt{3}$  unit cell can be noticed in the empty-state STM image in Fig. 2(b)]. When the transformation within the phase domains is completed, deposition of the additional In atoms results in the formation of the three-dimensional (3D) islands along the step edges as shown in Fig. 3.

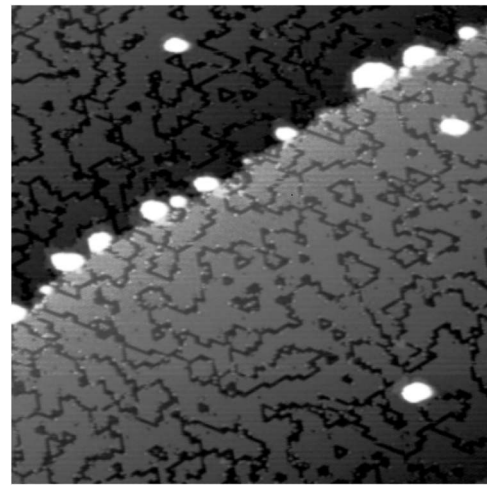


FIG. 3. Large-scale ( $100 \times 100 \text{ nm}^2$ ) empty-state (+2.3 V) STM image of the Si(111)- $\alpha$ - $\sqrt{3} \times \sqrt{3}$ -Au surface after RT deposition of 0.2 ML of In.

Figure 4 illustrates effect of the  $600^\circ\text{C}$  annealing on the structure of the RT-prepared (Au,In)/Si(111) interface. Note that this annealing temperature corresponds to the temperature, where the  $\alpha$ - $\sqrt{3} \times \sqrt{3} \leftrightarrow \gamma$ - $\sqrt{3} \times \sqrt{3}$  phase transition takes place.<sup>1-3</sup> Comparing the surfaces with 0.1 ML of In before and after annealing [Figs. 2(a) and 4(a), respectively], one can see that annealing results in coarsening of the  $\sqrt{3} \times \sqrt{3}$ -(Au,In) domains. Surface between the coarsened  $\sqrt{3} \times \sqrt{3}$ -(Au,In) domains looks disordered. It contains also small round islands of nearly equal size. The area fraction occupied by the  $\sqrt{3} \times \sqrt{3}$ -(Au,In) phase decreases with annealing from 0.35 to 0.27 due to the partial In desorption, which was indicated also by the decrease of the In Auger peak. Note that at  $600^\circ\text{C}$  In desorption is significant<sup>18,19</sup> (for example, upon annealing at  $600^\circ\text{C}$  for about 1 min In desorbs completely and the  $\alpha$ - $\sqrt{3} \times \sqrt{3}$ -Au surface restores upon cooling to RT).

With increasing In coverage, the domains of the  $\sqrt{3} \times \sqrt{3}$ -(Au,In) phase increase in size [see the Fig. 4(b) with 0.2 ML of In] and eventually at deposited In coverage of about 0.3 ML (and  $\sim 0.15$  ML of In left after annealing) the whole surface is occupied by the  $\sqrt{3} \times \sqrt{3}$ -(Au,In) phase [Fig. 4(c)]. In the latter case, the size of the  $\sqrt{3} \times \sqrt{3}$ -(Au,In) domains is as large as the terrace width, i.e., up to several hundreds nm, as shown in Fig. 5. In the same large-scale STM image, one can also notice the presence of the scarce 3D islands.

The obtained results can be interpreted as follows. Indium adsorption induces transformation of the  $\sqrt{3} \times \sqrt{3}$ -Au phase to the  $\sqrt{3} \times \sqrt{3}$ -(Au,In) phase. The transformation takes place already at room temperature. However, it is limited by the area occupied by the  $\sqrt{3} \times \sqrt{3}$ -Au domains and does not affect the domain-wall network. Moreover, the atomic structure of the domain walls plausibly remains unchanged. When transformation within domains is completed, the excess In atoms agglomerate into 3D islands. Annealing at  $600^\circ\text{C}$  is known to cause the “melting” of the domain walls.<sup>1</sup> As a result, coarsening of the  $\sqrt{3} \times \sqrt{3}$ -(Au,In) domains takes



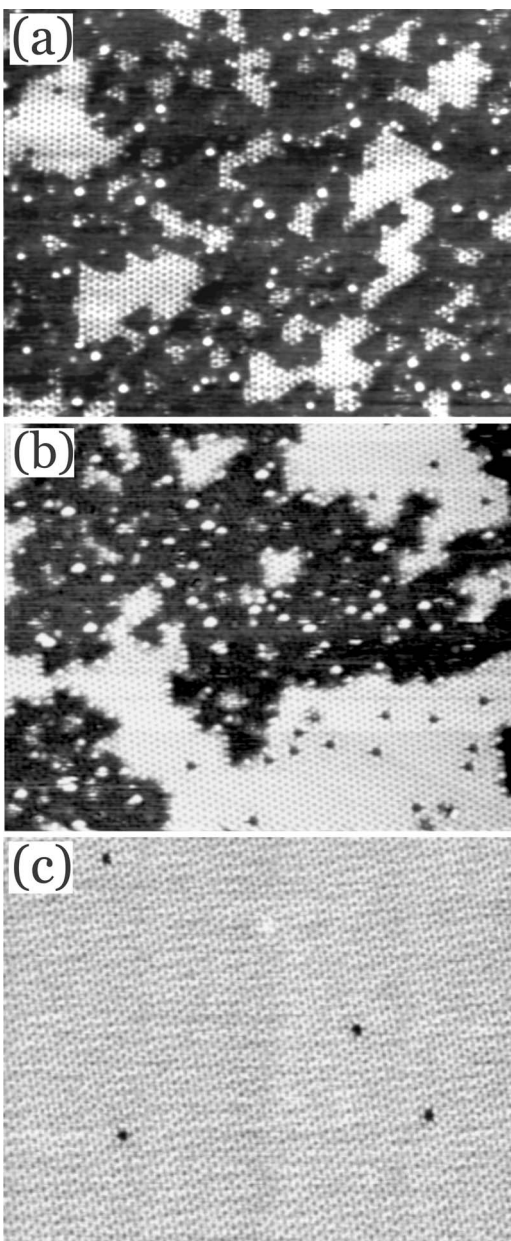


FIG. 4.  $50 \times 40 \text{ nm}^2$  filled-state ( $-2.0 \text{ V}$ ) STM images of the  $\text{Si}(111)\sqrt{3} \times \sqrt{3}\text{-(Au,In)}$  prepared by RT deposition of (a) 0.1, (b) 0.2, and (c) 0.4 ML of In, followed by annealing at  $600^\circ\text{C}$  for 15 s.

place. When the In amount is sufficient, the highly ordered homogeneous  $\sqrt{3} \times \sqrt{3}\text{-(Au,In)}$  phase occupies the whole surface. During annealing, the excess In atoms desorb from the surface. In turn, the excess Au atoms from the domain walls (recall that domain walls in the  $\alpha\text{-}\sqrt{3} \times \sqrt{3}\text{-Au}$  phase are heavy domain walls<sup>1,17</sup>) agglomerate into scarce 3D islands.

### B. Composition of $\text{Si}(111)\sqrt{3} \times \sqrt{3}\text{-(Au,In)}$ phase

Let us consider now the composition of the  $\text{Si}(111)\sqrt{3} \times \sqrt{3}\text{-(Au,In)}$  phase. No Si redistribution has been detected during transition from  $\alpha\text{-}\sqrt{3} \times \sqrt{3}\text{-Au}$  to  $\sqrt{3} \times \sqrt{3}\text{-(Au,In)}$ , which means that both surfaces has the

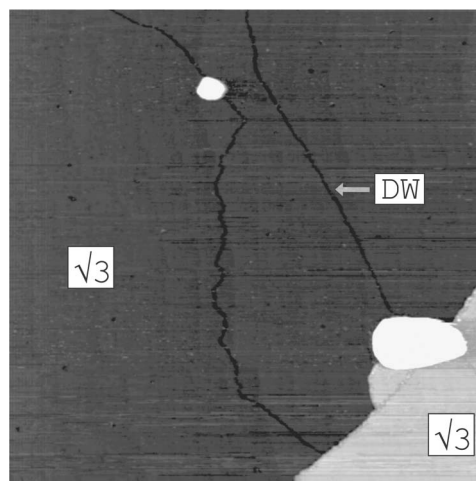


FIG. 5. Large-scale ( $400 \times 400 \text{ nm}^2$ ) filled-state ( $-2.3 \text{ V}$ ) STM image of the  $\text{Si}(111)\text{-}\alpha\text{-}\sqrt{3} \times \sqrt{3}\text{-Au}$  surface after RT deposition of 0.5 ML of In followed by annealing at  $600^\circ\text{C}$ .

same top Si atoms density. Our experimental determination based on the measurements of the area occupied by the islands in the two-level island-on-terrace system<sup>6</sup> yields the value of about 0.9 ML of Si for both surfaces. This is in agreement with the results of the earlier STM study,<sup>20</sup> in which the top Si atom density in the  $\alpha\text{-}\sqrt{3} \times \sqrt{3}\text{-Au}$  phase has been found to be about 1 ML from the hole-island analysis. Note that the CHCT model of the  $\sqrt{3} \times \sqrt{3}\text{-Au}$  phase suggests a missing-top layer structure of Si surface, i.e., also 1 ML of Si. So, it is safe to conclude that Si atom density of the  $\text{Si}(111)\sqrt{3} \times \sqrt{3}\text{-(Au,In)}$  phase is 1 ML.

As for the Au coverage of the  $\text{Si}(111)\sqrt{3} \times \sqrt{3}\text{-(Au,In)}$  phase, it is the same as in the ideal  $\sqrt{3} \times \sqrt{3}\text{-Au}$  phase. Though upon transformation scarce Au islands are observed (see Fig. 5), but these islands are due to the excess Au atoms accumulated originally in the heavy domain walls of the  $\alpha\text{-}\sqrt{3} \times \sqrt{3}\text{-Au}$  phase. The minimal amount of Au of  $1/3 \text{ ML}$  (i.e., one atom per each  $\sqrt{3} \times \sqrt{3}$  unit cell), which could be removed from the  $\sqrt{3} \times \sqrt{3}\text{-Au}$  domains, produces much higher density of islands, as was confirmed in a test experiment with calibrated Au deposition (not shown here). According to the CHCT model, an ideal  $\sqrt{3} \times \sqrt{3}\text{-Au}$  phase contains 1 ML of Au (one Au trimer per  $\sqrt{3} \times \sqrt{3}$  unit cell), which means that real  $\alpha\text{-}\sqrt{3} \times \sqrt{3}\text{-Au}$  surface should have Au coverage somewhat beyond 1 ML due to the presence of heavy domain walls. The Au trimer structure has been proved by ions scattering spectroscopy,<sup>21,22</sup> low-energy electron diffraction (LEED)  $I\text{-V}$  analysis,<sup>23</sup> scanned-energy glancing-angle Kikuchi electron spectroscopy,<sup>24</sup> x-ray standing-wave analysis,<sup>25</sup> and total-energy calculations.<sup>2,26</sup> However, in the number of studies it was indicated that the completed  $\alpha\text{-}\sqrt{3} \times \sqrt{3}\text{-Au}$  phase is observed at Au coverage of less than 1 ML (typically, around 0.7–0.8 ML),<sup>1,27–29</sup> which causes some doubts on the validity of the CHCT model. However, convincing model with  $2/3 \text{ ML}$  of Au is lacking. For the subsequent discussion, we accept the CHCT model as a basic model, which allows us a clear interpretation of all obtained results. However, strictly speaking, this fact cannot be considered as a proof of the validity of CHCT model.

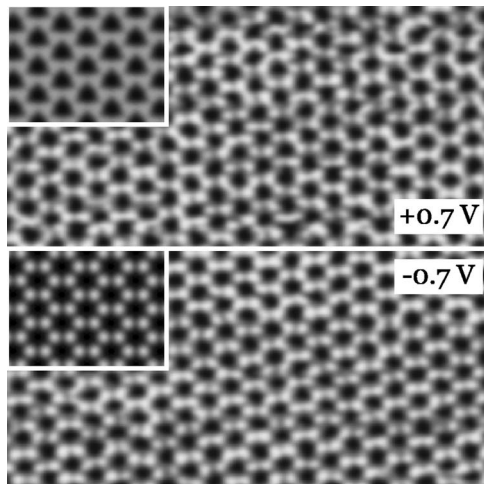


FIG. 6. High-resolution ( $12 \times 12 \text{ nm}^2$ ) dual-polarity ( $\pm 0.7 \text{ V}$ ) STM image of the Si(111) $\sqrt{3} \times \sqrt{3}$ -(Au,In) phase. Insets show the corresponding simulated STM images.

An intriguing question concerns the In coverage of the Si(111) $\sqrt{3} \times \sqrt{3}$ -(Au,In) phase. According to the Auger electron spectroscopy (AES) data, when the homogeneous  $\sqrt{3} \times \sqrt{3}$ -(Au,In) surface is formed,  $\sim 0.15 \text{ ML}$  of In is left at the surface after annealing (in this case, absolute amplitude of the In Auger peak is about a half of the peak amplitude from the Si(111) $\sqrt{3} \times \sqrt{3}$ -In surface). This corresponds to about 0.5 In atom (i.e., less than one In atom) per  $\sqrt{3} \times \sqrt{3}$  unit cell.

### C. Possible structure of Si(111) $\sqrt{3} \times \sqrt{3}$ -(Au,In) phase

Important questions for understanding atomic arrangement of the  $\sqrt{3} \times \sqrt{3}$ -(Au,In) phase are whether the basic CHCT structure is preserved or not and where In atoms are located. In order to answer these questions, we have conducted *ab initio* total-energy calculations, in which the effect of In adsorption on the stability of the Au trimers have been tested. There are only two reasonable high-symmetry sites within the  $\sqrt{3} \times \sqrt{3}$  unit cell for possible In adsorption. These are the  $T_4$  site in the center of the Au trimer and two equivalent free  $T_4$  sites (with respect to the first complete Si double layer). When In atom is placed in the center of the Au trimer, the trimer becomes broken. When In atom is placed in the free  $T_4$  site, the Au trimer is preserved with slight increasing of the trimer side from 0.284 to 0.290 nm. This configuration appears to be by 1.03 eV more stable than that with a broken Au trimer. Thus, the calculations demonstrate that the basic CHCT structure retains and In atoms occupy the free  $T_4$  sites. In the optimized model, In atoms occupying these sites were found to be located 0.18 nm higher than Au atoms, which means that In atoms should produce the dominant contribution to the STM images at both bias polarities.

The experimental high-resolution STM images demonstrate that at both polarities the  $\sqrt{3} \times \sqrt{3}$ -(Au,In) phase shows up as a honeycomb array of round bright protrusions, which location is the same both in the empty-state and filled-state STM images (Fig. 6). In order to elucidate their loca-

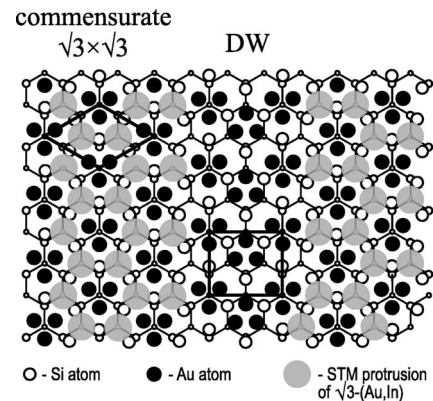


FIG. 7. Schematic diagram illustrating the location of the STM protrusions of the  $\sqrt{3} \times \sqrt{3}$ -(Au,In) phase superposed on the CHCT structure with a domain wall. Location of the STM protrusions coincides with the most stable adsorption sites of In atoms, as determined by calculations.

tion, we have considered the STM images like that shown in Fig. 2(b). As RT adsorption of In does not alter the domain-wall structure, the central protrusion in the  $2 \times \sqrt{3}$  domain-wall unit cell can be used as a reference point to tie the locations of the STM protrusions in the  $\sqrt{3} \times \sqrt{3}$ -Au and  $\sqrt{3} \times \sqrt{3}$ -(Au,In) phases to each other. Taking into account that according to the CHCT model the  $\sqrt{3} \times \sqrt{3}$ -Au protrusions correspond to the centers of the Au trimers,<sup>2</sup> this evaluation leads to the picture shown in Fig. 7. As one can see, in the  $\sqrt{3} \times \sqrt{3}$  unit cell the protrusions occupy the two free  $T_4$  sites with respect to the first complete Si double layer. Note that these are the most stable adsorption sites of In atoms, as revealed by calculations. This consistency between experiment and calculations is clearly illustrated by the close resemblance of the experimental and simulated STM images (Fig. 6).

However, the honeycomb arrangement seen in STM images implies the In coverage of  $2/3 \text{ ML}$  of In (two In atoms per  $\sqrt{3} \times \sqrt{3}$  unit cell), while actual In coverage is about 0.15 ML (about 0.5 In atom per  $\sqrt{3} \times \sqrt{3}$  unit cell). This contradiction can be resolved if one takes into account that according to our calculations the neighboring adsorption sites are separated by relatively low barrier of about 0.4 eV. This means that at RT the In atoms can freely hop from one adsorption site to another, visiting all of them. As a result, the STM images display the time-averaging picture, in which all sites are seen as being occupied. Our low-temperature STM observations have shown that the motion of In atoms can be frozen by cooling the sample, as illustrated in Fig. 8, showing the empty-state STM appearance of the Si(111) $\sqrt{3} \times \sqrt{3}$ -(Au,In) surface at 125 K. One can see that instead of the homogeneous honeycomb array seen at RT the surface shows up as small fragments of the hexagonal  $\sqrt{3} \times \sqrt{3}$  arrays of protrusions (i.e., with a single protrusion per  $\sqrt{3} \times \sqrt{3}$  unit cell). Direct counting of the protrusions yields the value of  $0.14 \pm 0.04 \text{ ML}$ , which coincides with the coverage of In atoms determined by AES. Absence of the honeycomb  $\sqrt{3} \times \sqrt{3}$  arrays demonstrates that In atoms actually avoid occupying the same  $\sqrt{3} \times \sqrt{3}$  unit cell simultaneously. The latter conclusion is in agreement with the re-



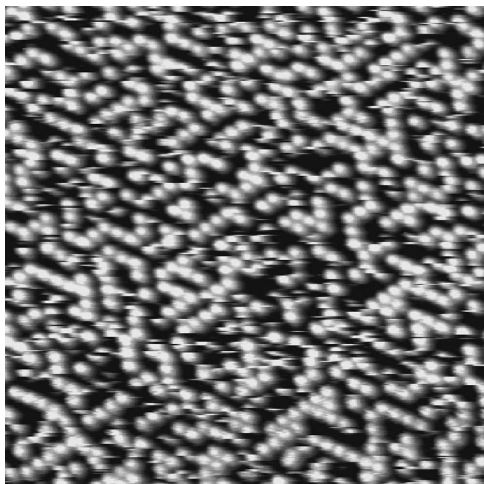


FIG. 8.  $25 \times 25 \text{ nm}^2$  empty-state (+1.9 V) STM image of the  $\text{Si}(111)\sqrt{3} \times \sqrt{3}\text{-(Au,In)}$  surface after cooling to 125 K.

sults of our calculations, in which the relative energies for In atoms at the CHCT  $\sqrt{3} \times \sqrt{3}\text{-Au}$  surface and in the In island have been compared. It has been found that for the first In atom in the  $\sqrt{3} \times \sqrt{3}$  unit cell occupation of the  $\sqrt{3} \times \sqrt{3}\text{-Au}$  surface is by 0.03 eV more preferable than the place within In island. But when the second atom is added to the  $\sqrt{3} \times \sqrt{3}$  unit cell, the place within an In island becomes by 0.2 eV more preferable.

Consider now a possible mechanism of the stabilization of the homogeneous  $\text{Si}(111)\sqrt{3} \times \sqrt{3}\text{-Au}$  surface by In adsorption. Occurrence of the network of the heavy domain walls at the original  $\text{Si}(111)\alpha\text{-}\sqrt{3} \times \sqrt{3}\text{-Au}$  surface indicates that stabilization of the CHCT structure in the interior of the domains requires an external compressive stress produced by excess Au atom density accumulated in the regions of the domain walls. It is believed that a similar effect could be produced by introducing into the Au adsorbate layer a certain amount of the second adsorbate, e.g., In. The required amount of In corresponds to the one when the compressive stress from the Au trimers is compensated by the tensile stress due to the adsorbed In atoms. According to our experimental results, this takes place at In coverage of about 0.15 ML. The results of calculations using approach described in Ref. 30 reproduce qualitatively the In-induced stress-relieving behavior. While original CHCT  $\sqrt{3} \times \sqrt{3}\text{-Au}$  surface has been found to be characterized by a stress of

+20.4 eV/nm<sup>2</sup>, addition of one In atom per  $\sqrt{3} \times \sqrt{3}$  unit cell has been determined to reduce the stress to +3.9 eV/nm<sup>2</sup>.

#### IV. CONCLUSION

Using scanning tunneling microscopy and total-energy calculations, we have studied the effect of In adsorption on the structure of the  $\text{Si}(111)\alpha\text{-}\sqrt{3} \times \sqrt{3}\text{-Au}$  phase. The obtained results demonstrate that In adsorption induces transformation of the  $\sqrt{3} \times \sqrt{3}\text{-Au}$  phase to the  $\sqrt{3} \times \sqrt{3}\text{-(Au,In)}$  phase. At room temperature, the transformation is limited by the interior of the original  $\sqrt{3} \times \sqrt{3}\text{-Au}$  domains and does not affect the domain-wall structure. Upon annealing at 600 °C, the domain walls are eliminated and highly ordered defect-free homogeneous  $\sqrt{3} \times \sqrt{3}\text{-(Au,In)}$  surface develops. The  $\sqrt{3} \times \sqrt{3}\text{-(Au,In)}$  phase contains 1 ML of Au, 1 ML of Si, and about 0.15 ML of In. It displays in the RT-STM images a honeycomb structure due to the In atoms hopping among the  $T_4$  adsorption sites in between Au trimers. The In atom motion is frozen at 125 K. We would like to remark that our results are comfortably understood within a framework of the CHCT model of the  $\text{Si}(111)\sqrt{3} \times \sqrt{3}\text{-Au}$  surface, but, strictly speaking, they cannot be considered as a solid argument in its favor.

The plausible mechanism of the stabilization of the domain-wall-free  $\text{Si}(111)\sqrt{3} \times \sqrt{3}\text{-(Au,In)}$  surface is the stress relief caused by In adsorption. This phenomenon might have a common nature and possibly could take place in many submonolayer system. Thus, the obtained results present the procedure to convert the surface with a high density of domain walls to the homogeneous surface free of domain walls. This conversion is believed to affect the surface electronic properties (especially, its conductivity) and in this respect  $\text{Si}(111)\sqrt{3} \times \sqrt{3}\text{-(Au,In)}$  surface could be an interesting object for such investigations. On the other hand, due to the absence of domain walls  $\text{Si}(111)\sqrt{3} \times \sqrt{3}\text{-(Au,In)}$  could also be of interest for the quantitative structural investigations, in particular, as an additional test for the CHCT model.

#### ACKNOWLEDGMENTS

Part of this work was supported by Russian Foundation for Basic Research (Grants Nos. 05-02-17824, 04-02-08242-ofi, 05-02-90571-nnc) and Russian Federation Ministry of Education and Science (Contract No. 02.434.11.2027).

\*Electronic address: gruznev@iacp.dvo.ru

<sup>1</sup>T. Nagao, S. Hasegawa, K. Tsuchie, S. Ino, C. Voges, G. Klos, H. Pfnür, and M. Henzler, *Phys. Rev. B* **57**, 10100 (1998).

<sup>2</sup>Y. G. Ding, C. T. Chan, and K. M. Ho, *Surf. Sci.* **275**, L691 (1992).

<sup>3</sup>E. A. Khramtsova and A. Ichimiya, *Phys. Rev. B* **57**, 10049 (1998).

<sup>4</sup>L. D. Marks, D. Grozea, R. Feidenhans'l, M. Nielsen, and R. L.

Johnson, *Surf. Rev. Lett.* **5**, 459 (1998).

<sup>5</sup>D. Grozea, E. Bengu, and L. D. Marks, *Surf. Sci.* **461**, 23 (2000).

<sup>6</sup>A. A. Saranin, A. V. Zotov, V. G. Lifshits, J. T. Ryu, O. Kubo, H. Tani, T. Harada, M. Katayama, and K. Oura, *Surf. Sci.* **429**, 127 (1999).

<sup>7</sup>J. L. Li, J. F. Jia, X. J. Liang, X. Liu, J. Z. Wang, Q. K. Xue, Z. Q. Li, J. S. Tse, Z. Zhang, and S. B. Zhang, *Phys. Rev. Lett.* **88**, 066101 (2002).

- <sup>8</sup>G. Le Lay, Surf. Sci. **132**, 169 (1983).
- <sup>9</sup>M. Beckstedte, A. Kley, J. Neugebauer, and M. Scheffler, Comput. Phys. Commun. **107**, 187 (1997).
- <sup>10</sup>R. Car and M. Parrinello, Phys. Rev. Lett. **55**, 2471 (1985).
- <sup>11</sup>D. M. Ceperley and B. J. Alder, Phys. Rev. Lett. **45**, 566 (1980).
- <sup>12</sup>J. P. Perdew and A. Zunger, Phys. Rev. B **23**, 5048 (1981).
- <sup>13</sup>N. Troullier and J. L. Martins, Phys. Rev. B **43**, 1993 (1991).
- <sup>14</sup>D. R. Hamann, Phys. Rev. B **40**, 2980 (1989).
- <sup>15</sup>M. Fuchs and M. Scheffler, Comput. Phys. Commun. **119**, 67 (1999).
- <sup>16</sup>J. Nogami, A. A. Baski, and C. F. Quate, Phys. Rev. Lett. **65**, 1611 (1990).
- <sup>17</sup>J. Falta, A. Hille, D. Novikov, G. Materlik, L. Seehofer, G. Falkenberg, and R. L. Johnson, Surf. Sci. **330**, L673 (1995).
- <sup>18</sup>S. Baba, M. Kawaji, and A. Kinbara, Surf. Sci. **85**, 29 (1979).
- <sup>19</sup>V. G. Lifshits, V. B. Akilov, B. K. Churusov, and Y. L. Gavriljuk, Surf. Sci. **222**, 21 (1989).
- <sup>20</sup>A. Shibata, Y. Kimura, and K. Takayanagi, Surf. Sci. **273**, L430 (1992).
- <sup>21</sup>K. Oura, M. Katayama, F. Shoji, and T. Hanawa, Phys. Rev. Lett. **55**, 1486 (1985).
- <sup>22</sup>M. Chester and T. Gustafsson, Surf. Sci. **256**, 135 (1991).
- <sup>23</sup>J. Quinn, F. Jona, and P. M. Marcus, Phys. Rev. B **46**, 7288 (1992).
- <sup>24</sup>I. H. Hong, D. K. Liao, Y. C. Chou, C. M. Wei, and S. Y. Tong, Phys. Rev. B **54**, 4762 (1996).
- <sup>25</sup>A. Saito, K. Izumi, T. Takahashi, and S. Kikuta, Phys. Rev. B **58**, 3541 (1998).
- <sup>26</sup>M. Murayama, T. Nakayama, and A. Natori, Jpn. J. Appl. Phys., Part 1 **40**, 6976 (2001).
- <sup>27</sup>J. H. Huang and R. S. Williams, Phys. Rev. B **38**, 4022 (1988).
- <sup>28</sup>T. Takami, D. Fukushi, T. Nakayama, M. Uda, and M. Aono, Jpn. J. Appl. Phys., Part 1 **33**, 3688 (1994).
- <sup>29</sup>T. Kadohira, J. Nakamura, and S. Watanabe, J. Surf. Sci. Technol. **2**, 146 (2004).
- <sup>30</sup>N. Moll, M. Scheffler, and E. Pehlke, Phys. Rev. B **58**, 4566 (1998).